Supplementary Methods

ScRNA-seq data collection and processing

We systematically collected cancer-related scRNA-seq datasets with more than 100 cells, including mRNA and lncRNA expression profiles, from CancerSEA (http://biocc.hrbmu.edu.cn/CancerSEA/) (1), which were used for single-cell lncRNA-associated ceRNA network construction. A total of 20 single-cell datasets across 12 cancer types were obtained from CancerSEA. We also collected cancer-related 'scRNA-seq' datasets from GEO with the following keywords: ('single cell' OR 'single-cell' OR 'single cells' OR 'single-cells') AND ('transcriptomics' OR 'transcriptome' OR 'RNA-seq' OR 'RNA-sequencing' OR 'RNA sequencing' OR 'scRNA-seq' OR 'scRNA seq') AND ('tumour' OR 'cancer' OR 'carcinoma' OR 'neoplasm' OR 'neoplastic'). We selected datasets wherein the number of cancer cells were over a 100, after quality control, and the expression profiles of the cells could be annotated and divided into mRNA and lncRNA expression profiles using GENCODE (release 34, GRCh38). If the original papers included malignant and non-malignant cells, we only retained the malignant cells. Considering the high technical noise of single cell expression profiles, we controlled for the quality of the single cells included in the database. We excluded cells that expressed fewer than 1,000 genes. Genes with a detectable expression in at least 1% of cells were retained. Finally, a total of 94,605 cancer cells derived from 40 single-cell datasets across 25 cancer types were used for the construction of single-cell ceRNA networks. For each dataset, we showed the cluster map of cell populations, constructed cellular-specific lncRNA-associated ceRNA networks for all cells in the dataset, showed the sub-cellular localisations of these ceRNAs, and characterised the functional state of each cell.

Functional annotation data collection

To distinguish the functional states of different cancer cells, we downloaded the characteristic gene sets corresponding to the 14 functional states from CancerSEA, including stemness, invasion, metastasis, proliferation, EMT, angiogenesis, apoptosis, cell cycle, differentiation, DNA damage, DNA repair, hypoxia, inflammation, and quiescence (1). Based on these signatures, the functional state of each cancer cell in the datasets were evaluated using GSVA package in R (2). The sub-cellular and extracellular vesicle locations of lncRNAs, miRNAs, and mRNAs were collected from related databases (3-7) and published literature. For pathway annotation, a total of 1,329 biological pathway gene sets from Kyoto Encyclopedia of Genes and Genomes, BioCarta, Reactome, and other biological pathway databases were collected from MSigDB (8). For annotation of biological function, a total of 5,917 gene sets representing different functional terms were collected from Gene Ontology (9). Ten classic cancer hallmark processes, including Self-Sufficiency in Growth Signals, Insensitivity to Antigrowth Signals, Evading Apoptosis, Limitless Replicative Potential, Sustained Angiogenesis, Tissue Invasion and Metastasis, Genome Instability and Mutation, Tumour Promoting Inflammation, Reprogramming Energy Metabolism, and Evading Immune Detection, were derived from a previous study (10). We manually curated gene sets of the ten cancer hallmark processes from the corresponding GO terms.

Construction of single cell ceRNA networks

We collected candidate ceRNA pairs from two databases: starBase v2.0 (11) and LncACTdb 2.0 (12), and used the common ceRNAs as candidates for regulation. A total of 108,668 candidate ceRNA regulations were collected. To verify whether these ceRNA pairs were

associated with each other in a single cell, we used a published method for cell-specific network construction based on probability theory to identify ceRNA networks in single cells (Figure S2A) (13). We assume that a ceRNA pair may have an association in some cells but not in other cells due to differences in cell types.

We determined whether lncRNAs and mRNAs were related in a cell by testing the statistical independence of the candidate ceRNA expression values in the same cell. For a ceRNA pair of x(mRNA) and y(lncRNA) in cell k, we calculated the following statistic:

$$\rho_{xy}{}^{k} = \frac{\sqrt{n-1} \bullet \left(n \bullet n_{xy}{}^{k} - n_{x}{}^{k} n_{y}{}^{k} \right)}{\sqrt{n_{x}{}^{k} n_{y}{}^{k} \left(n - n_{x}{}^{k} \right) \left(n - n_{y}{}^{k} \right)}}$$

where n is the total number of cells. $n_{\mathrm{x}}{}^{(k)}$ and $n_{y}{}^{(k)}$ are predetermined integers. We set $n_{\mathrm{x}}{}^{(k)} = n_{\mathrm{y}}{}^{(k)} = 0.1n$. We draw the first two boxes near x_k and y_k, based on the predetermined $n_{\mathrm{x}}{}^{(k)}$ and $n_{y}{}^{(k)}$, and then we have the third box, which is simply the intersection of the previous two boxes (Figure S2B). Thus, we can obtain the value of $n_{xy}{}^{(k)}$ by counting the plots in the third box.

If x and y are independent of each other, this statistic follows a standard normal distribution and the mean value and variance for the n cells are 0 and 1, respectively. Therefore, we can determine the significance of the x, y correlation with this statistic. $edge_{xy}{}^{(k)}$ is set to 1 in the network of cell k with a false discovery rate (FDR) < 0.05. We retained pairs that meet FDR < 0.05 for network construction in a single cell. The algorithm requires that single-cell datasets must have both mRNA and lncRNA expression profiles, and the number of cells is greater than 100. However, there is no strict requirement for the data type of scRNA-seq array. This method is not sensitive to the normalisation method and is suitable for various types of gene expression matrices.

In scRNA-seq data, the statistic may result in zero due to experimental errors, and is meaningless in biology and may produce errors in the data analysis. Hence, we treat the zeros in the following way (13): (1) If we cannot distinguish whether or not the zeros result from zero expression or the experimental errors, $edge_{xy}^{(k)}$ is set to 0 when $x_k = 0$ or $y_k = 0$ without the consideration of the statistic. (2) If we know that the zeros result from the zero expression, $edge_{xy}^{(k)}$ is determined by the statistic.

Classification of cancer single cells

Using the Seurat package in R (14,15), we clustered cells according to gene expression and ceRNA occurrence profiles. When clustering cells according to gene expression, we merged the mRNA and lncRNA expression profiles and clustered the cells with this combined expression profile. When clustering cells according to the ceRNA occurrence as the characteristic value, if a certain ceRNA pair showed a significant correlation to the cell type, the log(p) value was used instead. On the contrary, when the ceRNA pair showed no significant correlation to the cell type, the characteristic value was assigned to 0. Then, we obtained the characteristic matrix for clustering, wherein the rows indicated ceRNA pairs, and the columns indicated cells.

Manual curation of experimentally supported lncRNA-ceRNA regulations and lncRNA biomarkers

To collect high-confidence lncRNA-ceRNA associations and lncRNA biomarkers, we retrieved published literature from PubMed related to lncRNAs, ceRNAs, and biomarkers. We used the

following combination of key words “(miRNA sponge OR ceRNA OR miRNA decoy OR competing RNA OR antagomir OR miRNA mediated) AND (lncRNA)” to search the PubMed database. The experimentally supported lncRNA-ceRNA regulations were manually curated from these published articles by at least two researchers. Further, we used the following combination of key words “(circulating OR drug-resistant OR prognostic OR immune OR metastasis OR recurrence OR cell growth OR EMT OR apoptosis OR autophagy) AND (lncRNA)” to collect biomarker records. A biomarker was selected if the lncRNA had been experimentally verified to be related to a circulating, drug-resistant, or prognostic process. In this study, we manually collected experimentally supported ceRNAs and biological biomarkers through several steps, as previously described (12,16). Only datasets supported by evidence from high-confidence experiments, such as PCR, western blot, or luciferase reporter assay, and other reliable methods were considered. Finally, a total of 2,154 experimentally supported lncRNA-ceRNA regulations and 9,306 lncRNA biomarkers associated with drug resistance, circulation, survival, immunity, metastasis, recurrence, cell growth, EMT, apoptosis, and autophagy were manually curated from literature, and integrated into the LnCeCell database.

Functional analysis of lncRNA-associated ceRNAs

The CeRNA-Function and CeRNA-Hallmark sections were developed, as part of LnCeCell, to perform functional analyses of lncRNAs based on a “guilt-by-association” strategy. For lncRNAs, the corresponding downstream mRNA targets were used to perform a function enrichment analysis. LnCeCell performs a hypergeometric test to evaluate the significant enrichment in different functional contexts. If there are a total of *N* genes in the genome, of

which *S* is involved in the gene set under investigation, and there are a total of *M* interesting target genes for analysis, of which *x* are involved with the same function, then the P value can be calculated as:

$$P = 1 - \sum_{t=0}^{x} \frac{\binom{S}{t}\binom{N-S}{M-t}}{\binom{N}{M}}$$

Significantly enriched functions were defined at a level of P < 0.05 and were further illustrated as a bar graph of the –log10(P) values.

Survival analysis of ceRNA regulations

The CeRNA-Survival section performs Cox regression analyses and provides Kaplan-Meier survival curves for lncRNAs, miRNAs, mRNAs, and their contribution to the ceRNA networks. LnCeCell derives clinical follow-up information of 10,141 patients from TCGA and performs a univariate Cox regression analysis to evaluate the association between survival state and the expression level of each lncRNA-miRNA-mRNA member in a ceRNA interaction. A risk score model, which takes into account both the strength and positive/negative association between each competing RNA and probability of survival, was developed to evaluate the association between survival and expression in a certain cancer (12). For each patient, the risk score was calculated by linearly combining the ceRNA expression values weighted by the Cox regression coefficients:

$$Risk\ score = \sum_{i=1}^{n} \beta_i Exp(c_i)$$

where β_i is the Cox regression coefficient of an lncRNA, miRNA, or mRNA in a ceRNA interaction (indicated as c_i), *n* is the number of competing RNAs (n=3 in this study), and

$Exp(c_i)$ is the expression value of competing RNA c_i in the corresponding sample. The median and mean risk scores were used to divide the samples into high - and low-risk groups.

Supplementary Figures

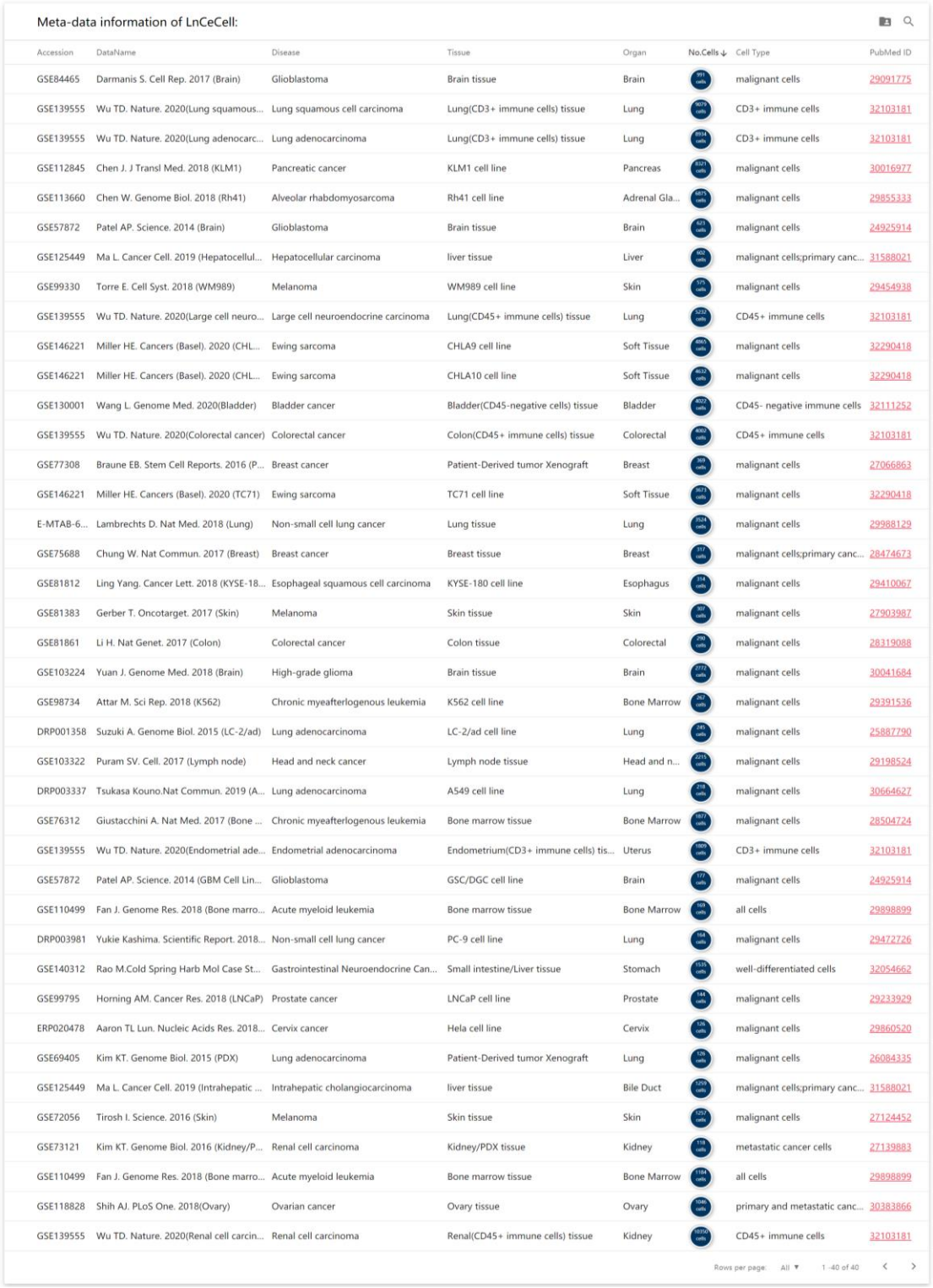

Meta-data information of LnCeCell:

Accession	DataName	Disease	Tissue	Organ	No.Cells	Cell Type	PubMed ID
GSE84465	Darmanis S. Cell Rep. 2017 (Brain)	Glioblastoma	Brain tissue	Brain	991 cells	malignant cells	29091775
GSE139555	Wu TD. Nature. 2020(Lung squamous...	Lung squamous cell carcinoma	Lung(CD3+ immune cells) tissue	Lung	9075 cells	CD3+ immune cells	32103181
GSE139555	Wu TD. Nature. 2020(Lung adenocarc...	Lung adenocarcinoma	Lung(CD3+ immune cells) tissue	Lung	8934 cells	CD3+ immune cells	32103181
GSE112845	Chen J. J Transl Med. 2018 (KLM1)	Pancreatic cancer	KLM1 cell line	Pancreas	8321 cells	malignant cells	30016977
GSE113660	Chen W. Genome Biol. 2018 (Rh41)	Alveolar rhabdomyosarcoma	Rh41 cell line	Adrenal Gla...	6875 cells	malignant cells	29855333
GSE57872	Patel AP. Science. 2014 (Brain)	Glioblastoma	Brain tissue	Brain	623 cells	malignant cells	24925914
GSE125449	Ma L. Cancer Cell. 2019 (Hepatocellul...	Hepatocellular carcinoma	liver tissue	Liver	602 cells	malignant cells;primary canc...	31588021
GSE99330	Torre E. Cell Syst. 2018 (WM989)	Melanoma	WM989 cell line	Skin	575 cells	malignant cells	29454938
GSE139555	Wu TD. Nature. 2020(Large cell neuro...	Large cell neuroendocrine carcinoma	Lung(CD45+ immune cells) tissue	Lung	5232 cells	CD45+ immune cells	32103181
GSE146221	Miller HE. Cancers (Basel). 2020 (CHL...	Ewing sarcoma	CHLA9 cell line	Soft Tissue	4965 cells	malignant cells	32290418
GSE146221	Miller HE. Cancers (Basel). 2020 (CHL...	Ewing sarcoma	CHLA10 cell line	Soft Tissue	4632 cells	malignant cells	32290418
GSE130001	Wang L. Genome Med. 2020(Bladder)	Bladder cancer	Bladder(CD45-negative cells) tissue	Bladder	4022 cells	CD45- negative immune cells	32111252
GSE139555	Wu TD. Nature. 2020(Colorectal cancer)	Colorectal cancer	Colon(CD45+ immune cells) tissue	Colorectal	4002 cells	CD45+ immune cells	32103181
GSE77308	Braune EB. Stem Cell Reports. 2016 (P...	Breast cancer	Patient-Derived tumor Xenograft	Breast	369 cells	malignant cells	27066863
GSE146221	Miller HE. Cancers (Basel). 2020 (TC71)	Ewing sarcoma	TC71 cell line	Soft Tissue	3673 cells	malignant cells	32290418
E-MTAB-6...	Lambrechts D. Nat Med. 2018 (Lung)	Non-small cell lung cancer	Lung tissue	Lung	3524 cells	malignant cells	29988129
GSE75688	Chung W. Nat Commun. 2017 (Breast)	Breast cancer	Breast tissue	Breast	317 cells	malignant cells;primary canc...	28474673
GSE81812	Ling Yang. Cancer Lett. 2018 (KYSE-18...	Esophageal squamous cell carcinoma	KYSE-180 cell line	Esophagus	314 cells	malignant cells	29410067
GSE81383	Gerber T. Oncotarget. 2017 (Skin)	Melanoma	Skin tissue	Skin	307 cells	malignant cells	27903987
GSE81861	Li H. Nat Genet. 2017 (Colon)	Colorectal cancer	Colon tissue	Colorectal	290 cells	malignant cells	28319088
GSE103224	Yuan J. Genome Med. 2018 (Brain)	High-grade glioma	Brain tissue	Brain	2772 cells	malignant cells	30041684
GSE98734	Attar M. Sci Rep. 2018 (K562)	Chronic myeafterlogenous leukemia	K562 cell line	Bone Marrow	267 cells	malignant cells	29391536
DRP001358	Suzuki A. Genome Biol. 2015 (LC-2/ad)	Lung adenocarcinoma	LC-2/ad cell line	Lung	245 cells	malignant cells	25887790
GSE103322	Puram SV. Cell. 2017 (Lymph node)	Head and neck cancer	Lymph node tissue	Head and n...	2215 cells	malignant cells	29198524
DRP003337	Tsukasa Kouno.Nat Commun. 2019 (A...	Lung adenocarcinoma	A549 cell line	Lung	218 cells	malignant cells	30664627
GSE76312	Giustacchini A. Nat Med. 2017 (Bone ...	Chronic myeafterlogenous leukemia	Bone marrow tissue	Bone Marrow	1877 cells	malignant cells	28504724
GSE139555	Wu TD. Nature. 2020(Endometrial ade...	Endometrial adenocarcinoma	Endometrium(CD3+ immune cells) tis...	Uterus	1809 cells	CD3+ immune cells	32103181
GSE57872	Patel AP. Science. 2014 (GBM Cell Lin...	Glioblastoma	GSC/DGC cell line	Brain	177 cells	malignant cells	24925914
GSE110499	Fan J. Genome Res. 2018 (Bone marro...	Acute myeloid leukemia	Bone marrow tissue	Bone Marrow	169 cells	all cells	29898899
DRP003981	Yukie Kashima. Scientific Report. 2018...	Non-small cell lung cancer	PC-9 cell line	Lung	168 cells	malignant cells	29472726
GSE140312	Rao M.Cold Spring Harb Mol Case St...	Gastrointestinal Neuroendocrine Can...	Small intestine/Liver tissue	Stomach	1535 cells	well-differentiated cells	32054662
GSE99795	Horning AM. Cancer Res. 2018 (LNCaP)	Prostate cancer	LNCaP cell line	Prostate	144 cells	malignant cells	29233929
ERP020478	Aaron TL Lun. Nucleic Acids Res. 2018...	Cervix cancer	Hela cell line	Cervix	126 cells	malignant cells	29860520
GSE69405	Kim KT. Genome Biol. 2015 (PDX)	Lung adenocarcinoma	Patient-Derived tumor Xenograft	Lung	126 cells	malignant cells	26084335
GSE125449	Ma L. Cancer Cell. 2019 (Intrahepatic ...	Intrahepatic cholangiocarcinoma	liver tissue	Bile Duct	1259 cells	malignant cells;primary canc...	31588021
GSE72056	Tirosh I. Science. 2016 (Skin)	Melanoma	Skin tissue	Skin	1257 cells	malignant cells	27124452
GSE73121	Kim KT. Genome Biol. 2016 (Kidney/P...	Renal cell carcinoma	Kidney/PDX tissue	Kidney	118 cells	metastatic cancer cells	27139883
GSE110499	Fan J. Genome Res. 2018 (Bone marro...	Acute myeloid leukemia	Bone marrow tissue	Bone Marrow	1184 cells	all cells	29898899
GSE118828	Shih AJ. PLoS One. 2018(Ovary)	Ovarian cancer	Ovary tissue	Ovary	1045 cells	primary and metastatic canc...	30383866
GSE139555	Wu TD. Nature. 2020(Renal cell carcin...	Renal cell carcinoma	Renal(CD45+ immune cells) tissue	Kidney	1035 cells	CD45+ immune cells	32103181

Rows per page: All ▾ 1-40 of 40 < >

Figure S1. ScRNA-seq meta-data information of LnCeCell.

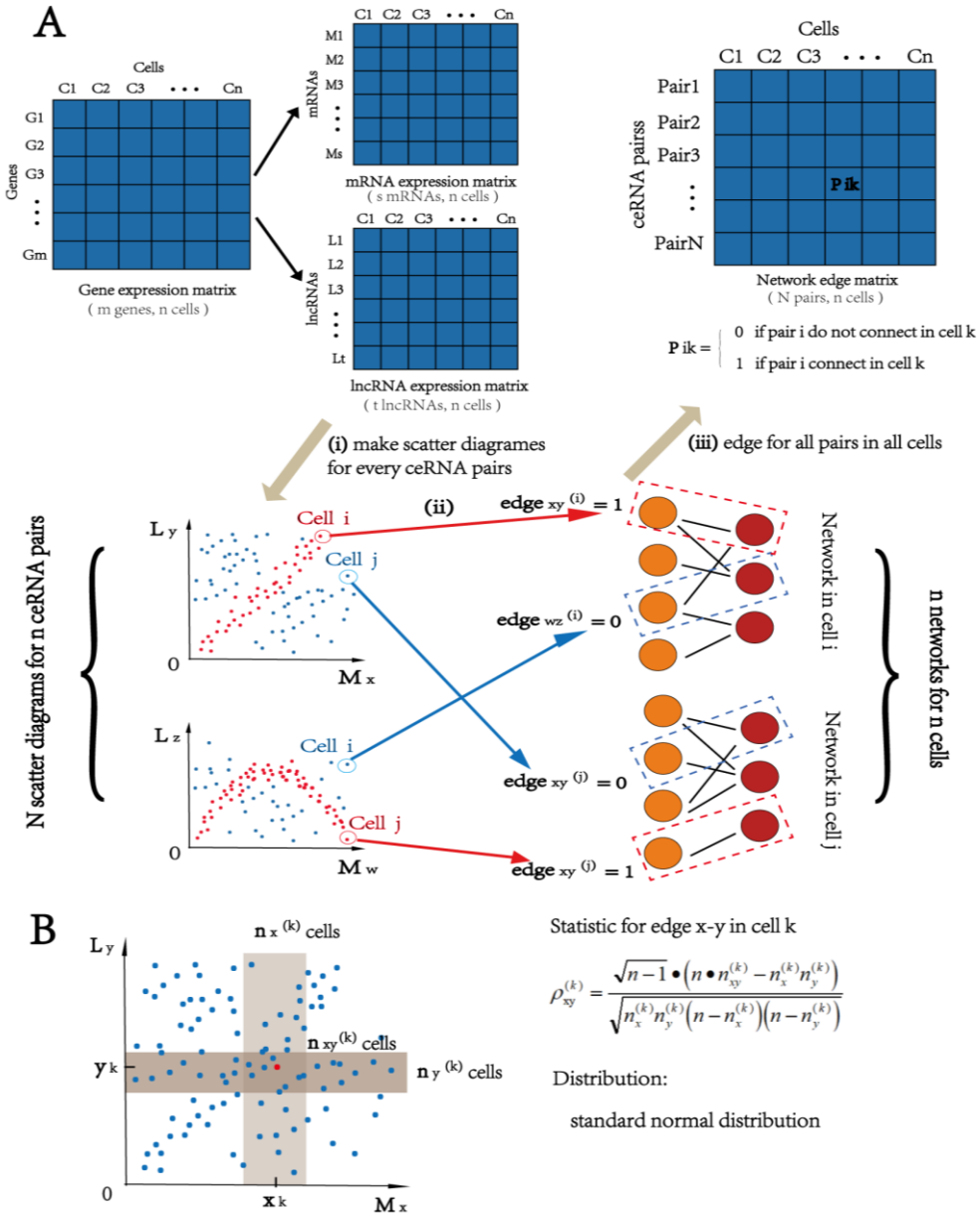

Figure S2. Single cell ceRNA networks construction and our statistical model. **(A)** Single cell ceRNA networks construction. (i) Scatter diagrams for every ceRNA pair, wherein each point represents a cell, and x- and y-values are the expression values of mRNA and lncRNA respectively in the n cells. Then N ceRNA pairs lead to N scatter diagrams. (ii) In the scatter diagram of mRNA (x) and lncRNA (y), a red plot signifies an edge between x and y in the cell-specific network, based on our statistical model, and a blue plot signifies no edge. We can then construct n cell-specific networks corresponding to n cells. (iii) We get the ceRNA occurrence profile, comprised of N rows and n columns. If pair i is connected in cell k, $P_{ik}=1$; or else, $P_{ik}=0$. **(B)** Our statistical model for the edge between mRNA: x and lncRNA: y. Near

the plot or cell k, the light and medium grey boxes represent the neighbourhood of x_k and y_k respectively. The intersection of the two boxes is the dark grey box, which represents the neighbourhood of (x_k, y_k). The number of plots in the light, medium and dark grey boxes is $n_x^{(k)}$, $n_y^{(k)}$ and $n_{xy}^{(k)}$ respectively. The statistic is designated as $\rho_{xy}^{(k)}$.If x and y are independent of each other, the statistic follows standard normal distribution. If the statistic $\rho_{xy}^{(k)}$ is significantly larger, there is an edge between x and y in cell k; otherwise there is no edge.

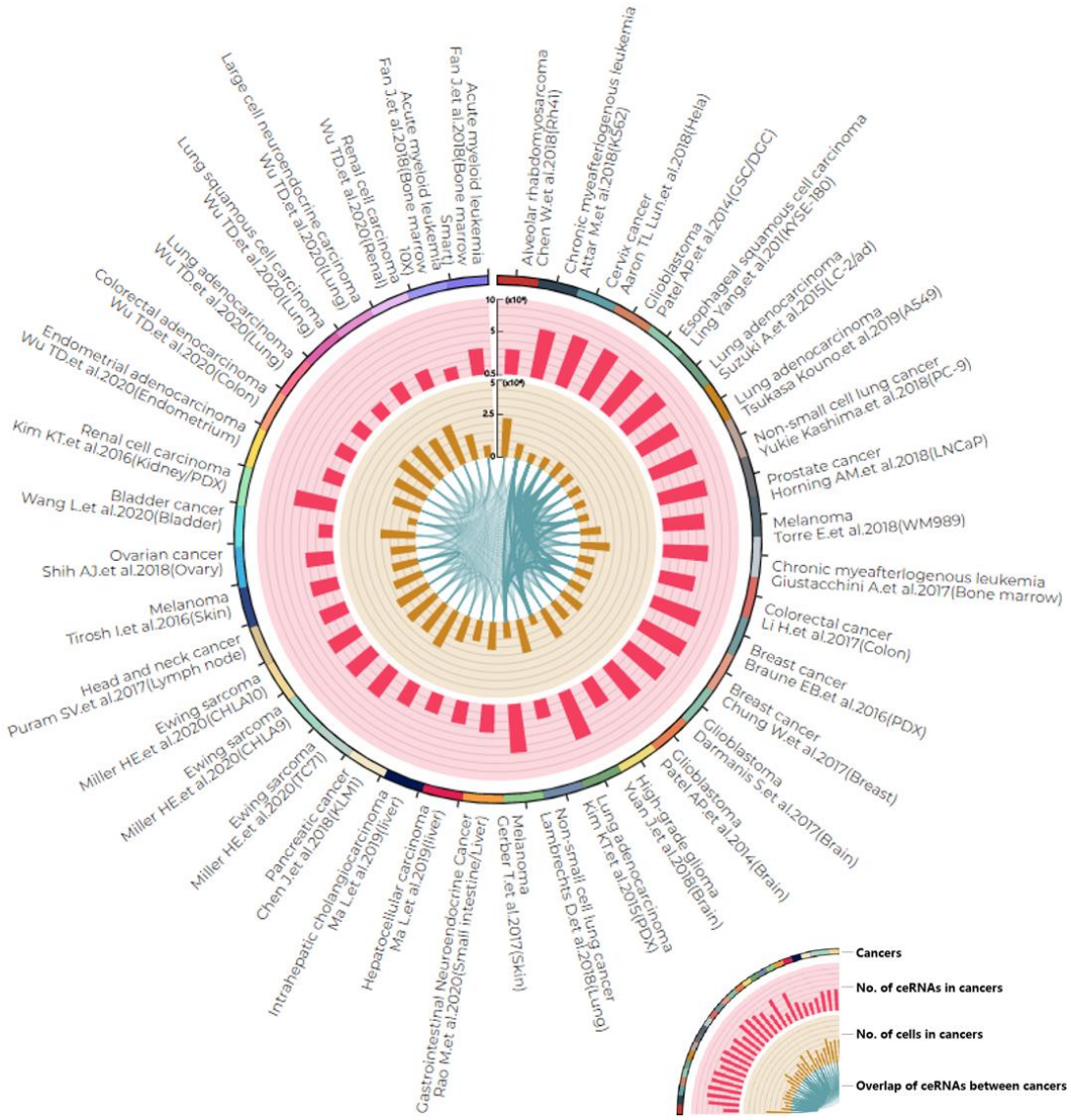

Figure S3. Comparison analysis of cells and ceRNAs across all 40 single-cell datasets. The bar graph indicates the number of ceRNAs and cells in different cancers. The links indicate the ceRNA overlap between different cancers.

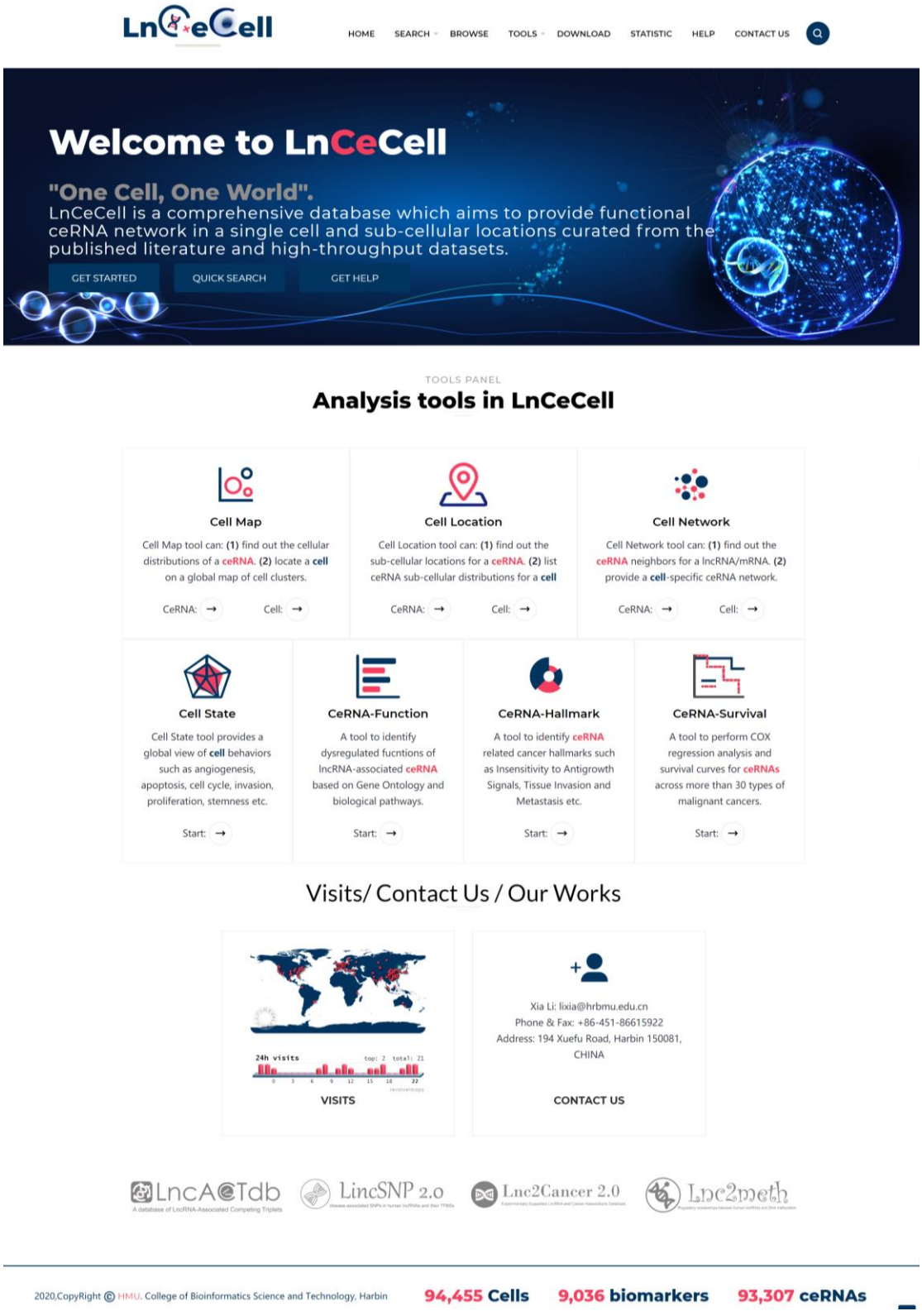

Figure S4. A screenshot of LnCeCell 'HOME' page.

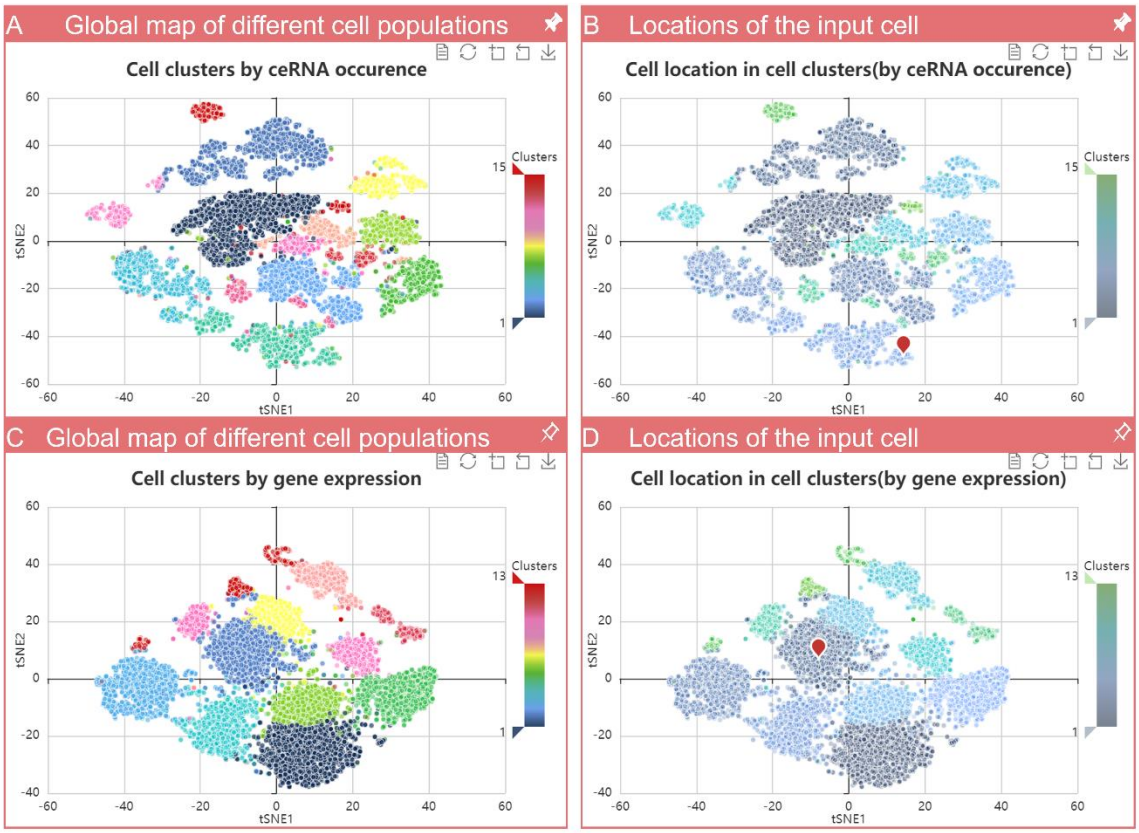

Figure S5. Cell location results of LnCeCell database. **(A)** Global map of different cell populations clustered by ceRNA occurrence in cells. **(B)** Location of the input cell in different populations clustered by ceRNA occurrence. **(C)** Global map of different cell populations clustered by gene expression in cells. **(D)** Location of the input cell in different populations clustered by gene expression.

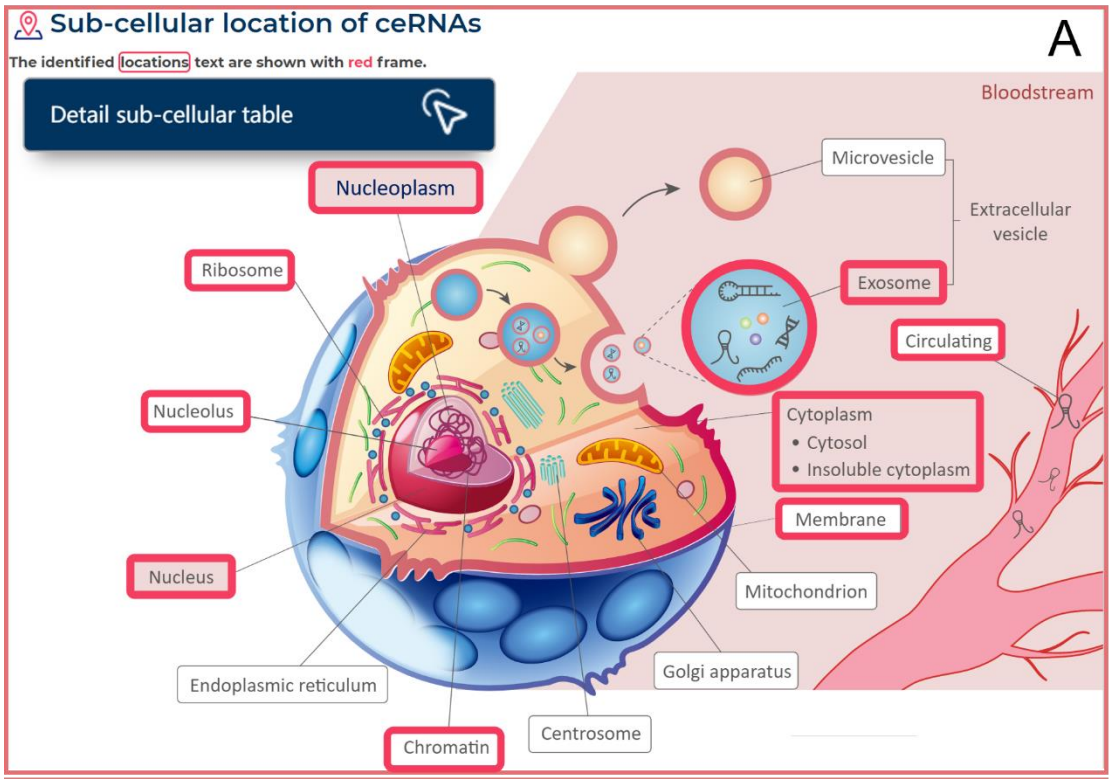

B

Location	ID	Name	Tissue	Source
ribosome	ENSG00000153363	LINC00467	Colon cancer cell	24393600
ribosome	ENSG00000179743	FLJ37453	Colon cancer cell	24393600
ribosome	ENSG00000226419	SLC16A1-AS1	K562 cells	27090285
ribosome	ENSG00000244879	GABPB1-AS1	K562 cells	27090285
ribosome	ENSG00000245937	LINC01184	Colon cancer cell	24393600
ribosome	ENSG00000246067	RAB30-AS1	Colon cancer cell	24393600
ribosome	ENSG00000246067	RAB30-AS1	K562 cells	27090285
ribosome	ENSG00000247092	SNHG10	K562 cells	27090285
ribosome	ENSG00000251562	MALAT1	Colon cancer cell	24393600
ribosome	ENSG00000256073	URB1-AS1	Colon cancer cell	24393600

Rows per page: 10 ▼ 1 -10 of 666

Figure S6. Sub-cellular locations of the ceRNAs in single cell. **(A)** A global view of possible sub-cellular locations of all ceRNAs which were associated with this cell. **(B)** Detailed sub-cellular location information including ceRNA names/IDs, possible locations, identified tissues/cell lines and data source.

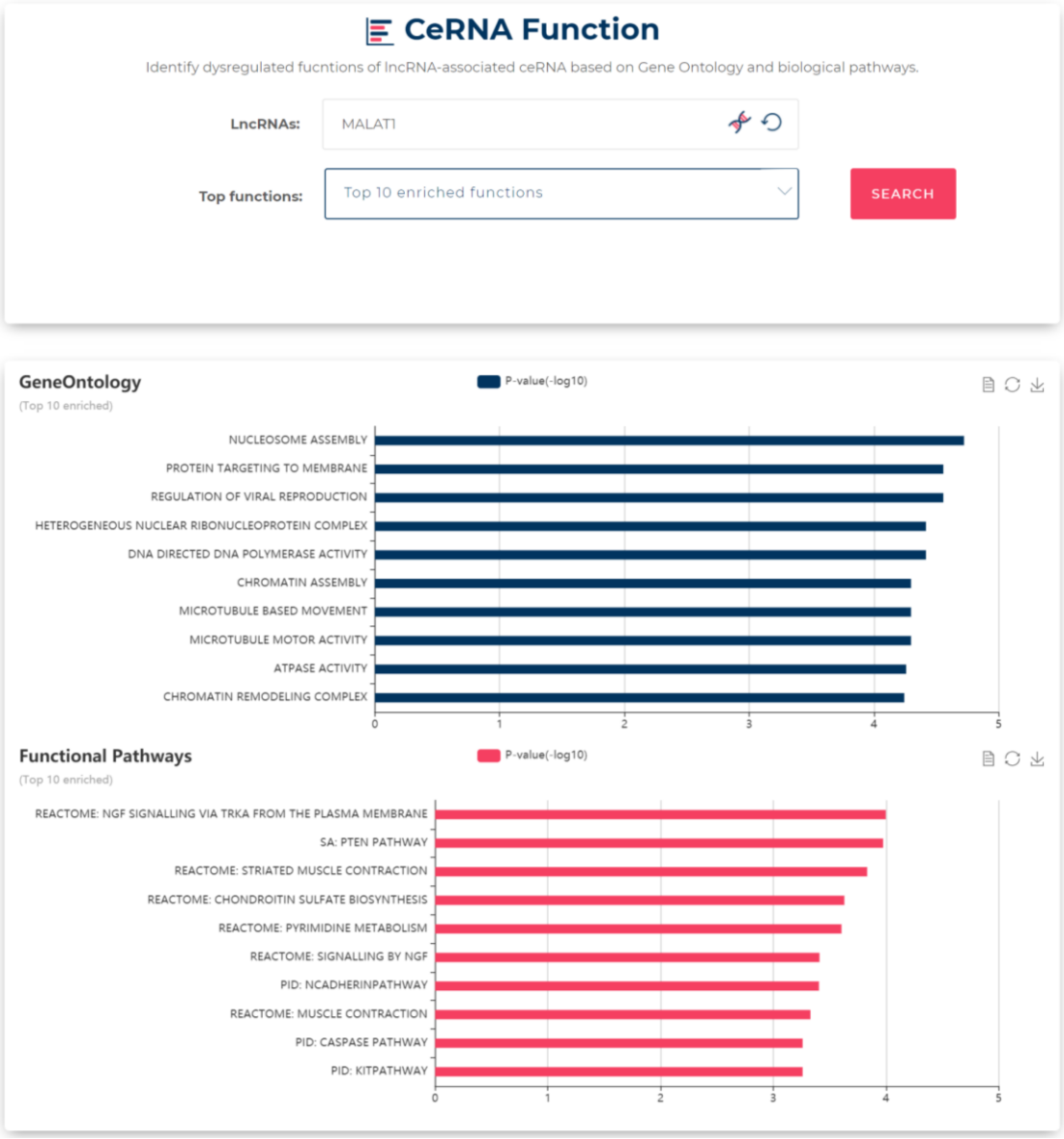

Figure S7. A screenshot of the CeRNA-Function tool in LnCeCell. Using this tool, users can infer ceRNA functions based on biological pathways and GO terms.

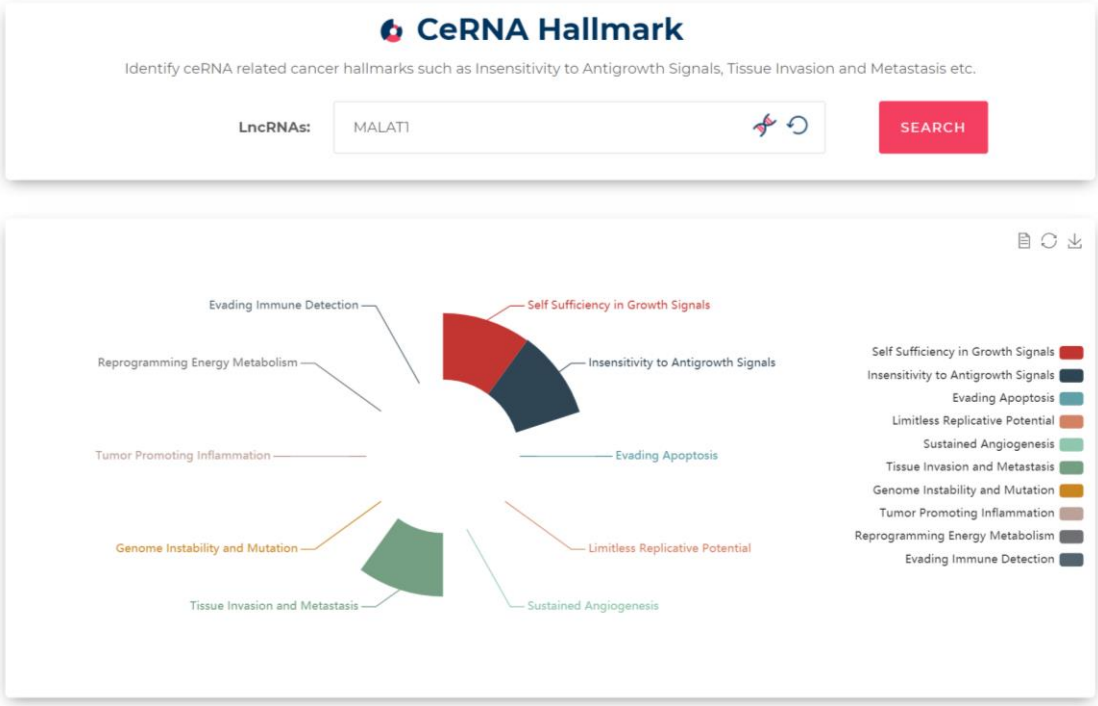

Figure S8. A screenshot of the CeRNA-Hallmark tool in LnCeCell. Using this tool, users can identify ceRNA-related cancer hallmarks such as "Insensitivity to Antigrowth Signals" and "Tissue Invasion and Metastasis".

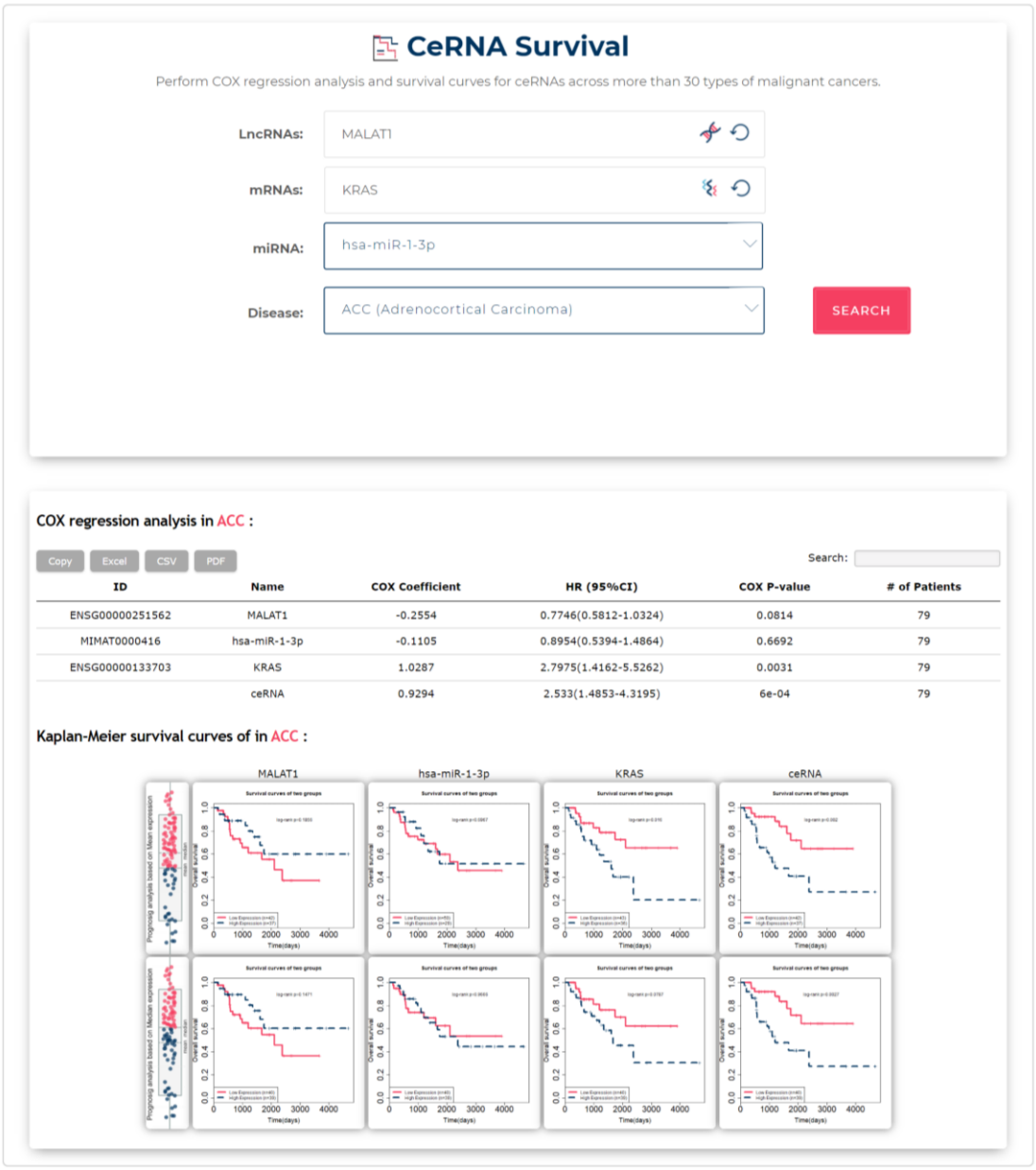

Figure S9. A screenshot of the CeRNA-Survival tool in LnCeCell. Using this tool, users can perform Cox survival analysis and obtain Kaplan-Meier curves of a ceRNA interaction across 33 types of TCGA cancers.

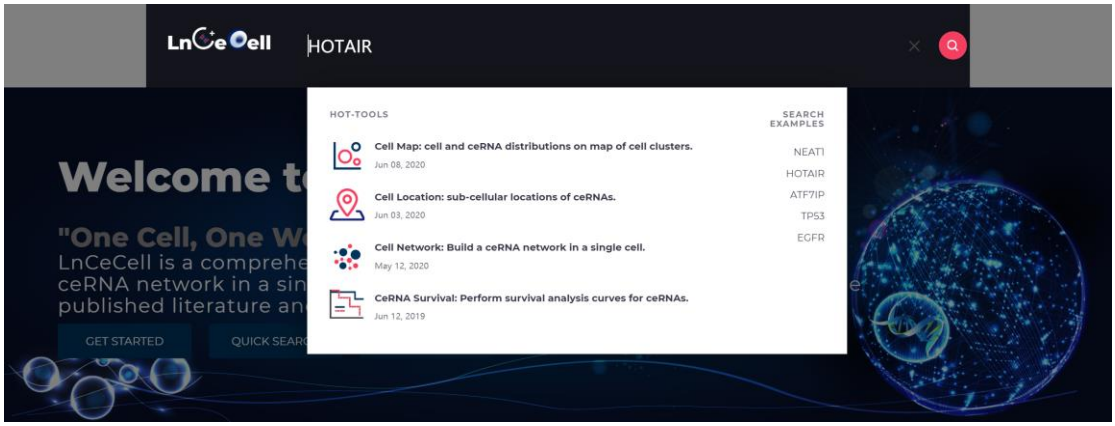

Figure S10. A screenshot of ‘QUICK SEARCH’ page in LnCeCell.

Figure S11. An example of ceRNA *MALAT1-KRAS* in pan-cancers. The layer with blue bars indicates the percentage of cells in which the *MALAT1-KRAS* can be identified in different cancer datasets. The layers with red and yellow bars indicate the number of ceRNAs and cells across different datasets, respectively. The inner links indicate the ceRNA overlap between different cancers.

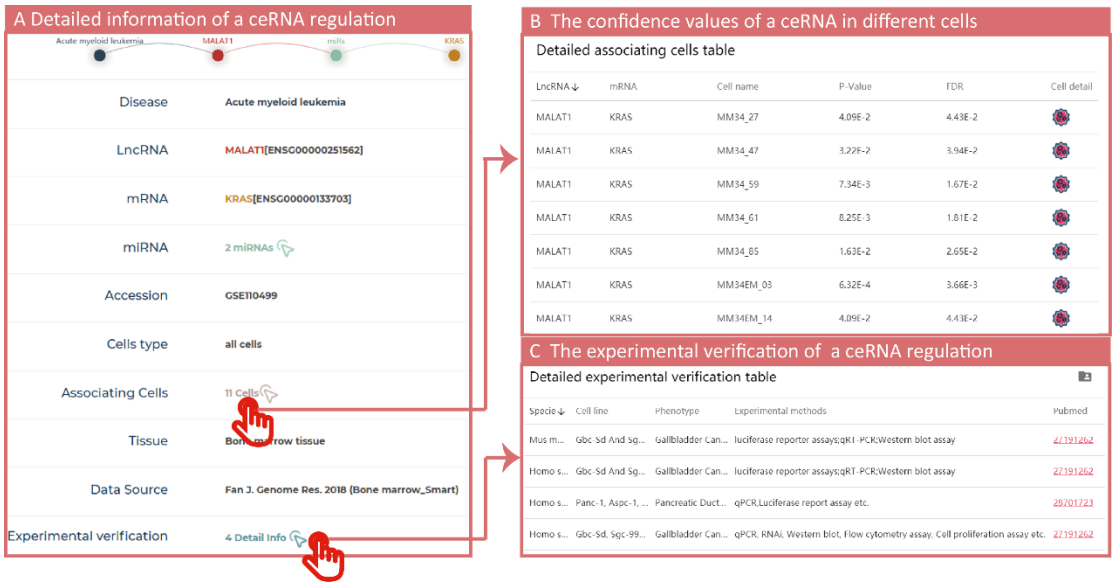

Figure S12. Related annotation of ceRNA regulation. (A) Detailed information of a ceRNA regulation. (B) The confidence values of a ceRNA in different cells. (C) The experimental verification of a ceRNA regulation.

References of Supplementary Methods

1. Yuan, H., Yan, M., Zhang, G., Liu, W., Deng, C., Liao, G., Xu, L., Luo, T., Yan, H., Long, Z. *et al.* (2019) CancerSEA: a cancer single-cell state atlas. *Nucleic Acids Res*, **47**, D900-d908.
2. Hänzelmann, S., Castelo, R. and Guinney, J. (2013) GSVA: gene set variation analysis for microarray and RNA-seq data. *BMC bioinformatics*, **14**, 7.
3. Li, S., Li, Y., Chen, B., Zhao, J., Yu, S., Tang, Y., Zheng, Q., Li, Y., Wang, P., He, X. *et al.* (2018) exoRBase: a database of circRNA, lncRNA and mRNA in human blood exosomes. *Nucleic Acids Res*, **46**, D106-d112.
4. Liu, T., Zhang, Q., Zhang, J., Li, C., Miao, Y.R., Lei, Q., Li, Q. and Guo, A.Y. (2019) EVmiRNA: a database of miRNA profiling in extracellular vesicles. *Nucleic Acids Res*, **47**, D89-d93.
5. Mas-Ponte, D., Carlevaro-Fita, J., Palumbo, E., Hermoso Pulido, T., Guigo, R. and Johnson, R. (2017) LncATLAS database for subcellular localization of long noncoding RNAs. *RNA*, **23**, 1080-1087.
6. Quek, X.C., Thomson, D.W., Maag, J.L., Bartonicek, N., Signal, B., Clark, M.B., Gloss, B.S. and Dinger, M.E. (2015) lncRNAdb v2.0: expanding the reference database for functional long noncoding RNAs. *Nucleic Acids Res*, **43**, D168-173.
7. Xia, S., Feng, J., Chen, K., Ma, Y., Gong, J., Cai, F., Jin, Y., Gao, Y., Xia, L., Chang, H. *et al.* (2018) CSCD: a database for cancer-specific circular RNAs. *Nucleic Acids Res*, **46**, D925-d929.
8. Liberzon, A., Birger, C., Thorvaldsdottir, H., Ghandi, M., Mesirov, J.P. and Tamayo, P. (2015) The Molecular Signatures Database (MSigDB) hallmark gene set collection. *Cell systems*, **1**, 417-425.
9. The Gene Ontology, C. (2019) The Gene Ontology Resource: 20 years and still GOing strong. *Nucleic acids research*, **47**, D330-D338.
10. Hanahan, D. and Weinberg, R.A. (2011) Hallmarks of cancer: the next generation. *Cell*, **144**, 646-674.
11. Li, J.H., Liu, S., Zhou, H., Qu, L.H. and Yang, J.H. (2014) starBase v2.0: decoding miRNA-ceRNA, miRNA-ncRNA and protein-RNA interaction networks from large-scale CLIP-Seq data. *Nucleic Acids Res*, **42**, D92-97.
12. Wang, P., Li, X., Gao, Y., Guo, Q., Wang, Y., Fang, Y., Ma, X., Zhi, H., Zhou, D., Shen, W. *et al.* (2019) LncACTdb 2.0: an updated database of experimentally supported ceRNA interactions curated from low- and high-throughput experiments. *Nucleic Acids Res*, **47**, D121-D127.
13. Dai, H., Li, L., Zeng, T. and Chen, L. (2019) Cell-specific network constructed by single-cell RNA sequencing data. *Nucleic Acids Res*, **47**, e62.
14. Butler, A., Hoffman, P., Smibert, P., Papalexi, E. and Satija, R. (2018) Integrating single-cell transcriptomic data across different conditions, technologies, and species. *Nature biotechnology*, **36**, 411-420.
15. Stuart, T., Butler, A., Hoffman, P., Hafemeister, C., Papalexi, E., Mauck, W.M., 3rd, Hao, Y., Stoeckius, M., Smibert, P. and Satija, R. (2019) Comprehensive Integration of Single-Cell Data. *Cell*, **177**, 1888-1902.e1821.
16. Gao, Y., Wang, P., Wang, Y., Ma, X., Zhi, H., Zhou, D., Li, X., Fang, Y., Shen, W., Xu, Y. *et al.* (2019) Lnc2Cancer v2.0: updated database of experimentally supported long non-coding RNAs in human cancers. *Nucleic acids research*, **47**, D1028-D1033.